

# APPLIED FORECASTING METHODS

Prof. Pritam Anand

## I. ABSTARCTION

This report takes a deep dive into Canadian oil production from 1973 to 2021, focusing on long-term trends and seasonal patterns. Over nearly five decades, the data shows a steady rise in production, alongside clear seasonal shifts—typically peaking in the winter months and dipping in the spring. By breaking down the data using time series decomposition, we were able to separate the trend, seasonal, and irregular components. This approach highlights just how powerful these analytical tools can be in uncovering the hidden patterns that shape energy production over time.

## II. PROBLEM STATEMENT

Time series data, like oil production figures, often reflect a mix of underlying influences—long-term trends, seasonal shifts, and short-term fluctuations. To truly understand what's driving these numbers, especially in a sector as critical as energy, it's important to look beneath the surface.

This analysis takes a closer look at Canadian oil production over the last fifty years, exploring a few key questions:

- How has oil production in Canada changed over time?
- Are there seasonal trends in the production cycle?
- Can we break down the data into meaningful components to better understand what's going on?
- And most importantly, what can we learn from analyzing these components individually?

By using time series decomposition, we can untangle the data into parts that make sense on their own—revealing clearer patterns and helping us see the bigger picture. For anyone involved in energy market analysis, production forecasting, or policy planning, these insights can be a game-changer.

## III. DATASET DESCRIPTION

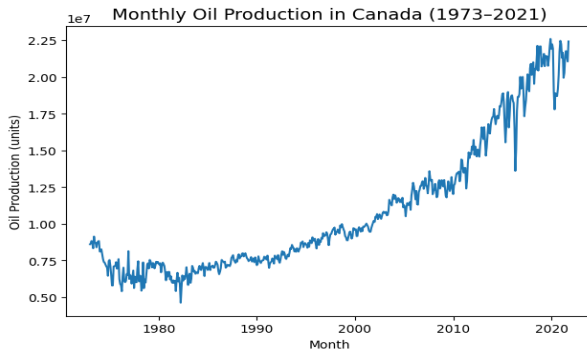


Fig. 1: Dataset

The dataset consists of monthly oil production figures for Canada spanning from January 1973 to October 2021, encompassing nearly 50 years of production history. The data includes:

- Country name (Canada for all entries as dataset focus on Canada only)
- Month (datetime format)
- Monthly oil production (measured in volume units)

The dataset contains 586 monthly observations with no missing values. Production volumes range from a minimum of 4,621,000 units to a maximum of 22,600,000 units, with a mean value of approximately 10,849,550 units and a standard deviation of 4,562,185 units. This wide range indicates substantial changes in production capacity over the observed period.

The data is structured as a time series with regular monthly intervals, making it suitable for temporal analysis techniques. The complete date range spans from January 1, 1973, to October 1, 2021, providing comprehensive coverage of Canada's oil production history through various economic cycles and technological developments.

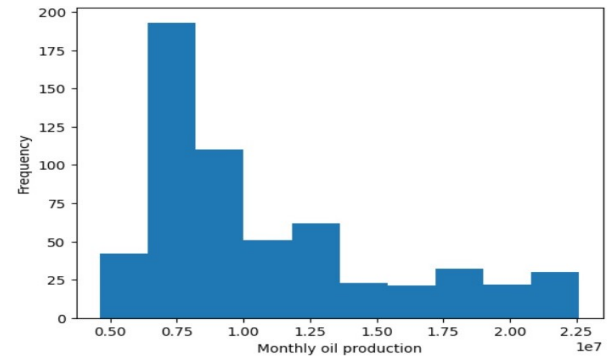


Fig. 2: Histogram plot for Dataset

The histogram shows the distribution of monthly oil production values. Most observations fall between 7 and 10 million units, with fewer months at higher production levels. The distribution is right-skewed, indicating a long tail toward higher production volumes.

## IV. METHOLOGY

### A. Decomposition

The decomposition of the monthly oil production data reveals a clear and persistent upward trend, indicating that Canada's oil output has steadily increased over the decades.

Seasonal Decomposition of Monthly Canadian Oil Production

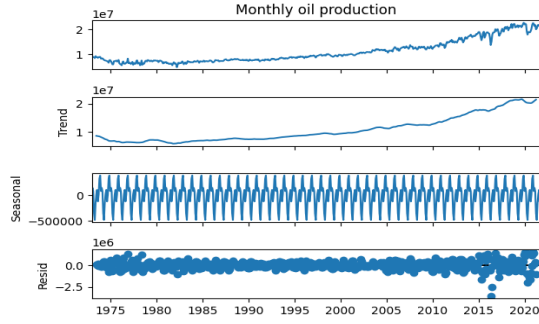


Fig. 3: Histogram plot for Dataset

Additionally, a strong seasonal pattern is evident, with production consistently peaking during certain months each year and dipping during others. This combination of long-term growth and regular seasonality highlights both structural expansion in the industry and recurring operational or environmental influences on production levels.

### B. Stationary Check

The Augmented Dickey-Fuller (ADF) test results confirm our observations from the decomposition analysis. The original time series has an ADF statistic of 2.024635 with a high p-value of 0.998704, strongly indicating non-stationarity. This aligns with the clear upward trend visible in our decomposition plot. After applying first differencing, the ADF statistic becomes significantly negative (-5.661735) with a p-value near zero (0.000001), confirming that the differenced series is stationary. This transformation is essential for accurate time series forecasting, as most forecasting models require stationary data. The first-order differencing effectively removes the long-term trend component that dominated the original series.

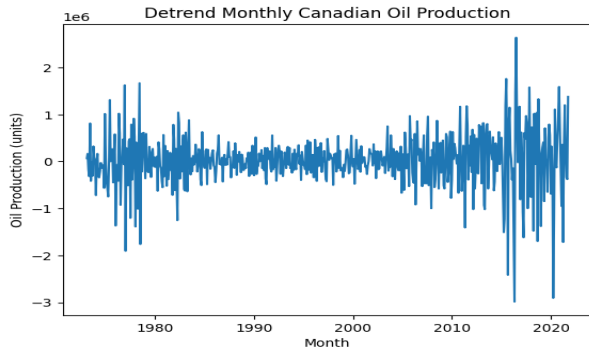


Fig. 4: First difference plot

The detrended time series analysis reveals an important characteristic of our Canadian oil production data: while first differencing successfully addressed the non-stationarity issue (as confirmed by the ADF test results with p-value of 0.000001), the variance of the differenced series exhibits heteroscedasticity. The variance pattern shows a distinct evolution - initially decreasing, then stabilizing temporarily, before

increasing in more recent periods. This changing variance violates a key assumption for many time series forecasting models, which require both constant mean and constant variance.

To address this heteroscedasticity, a logarithmic transformation is appropriate before differencing. This approach is particularly suitable for our oil production data for several reasons. First, logarithmic transformations are effective when variance is proportional to the level of the series, which appears to be the case as production volumes grew substantially over the decades. The transformation will compress the higher values and expand the lower values, effectively stabilizing the variance across the entire series.

By applying the log transformation followed by differencing, we create a series that better satisfies the stationarity requirements of both constant mean and constant variance, providing a more reliable foundation for forecasting models like ARIMA. This stabilization is crucial for obtaining valid confidence intervals and improving overall forecast accuracy as we project future Canadian oil production levels.

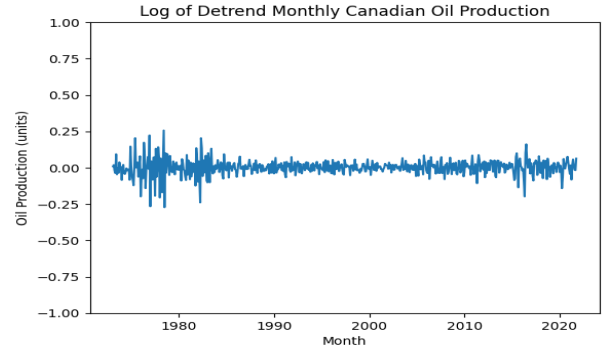


Fig. 5: Log First difference plot

From the above we can say that variance is almost constant.

### C. ACF and PACF

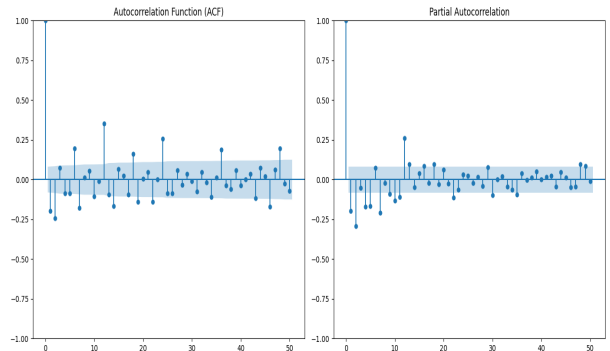


Fig. 6: Autocorrelation and Partial Autocorrelation plots

The ACF and PACF analysis of our log-transformed and differenced oil production data reveals a crucial pattern that guides our modeling approach. The absence of gradually decaying or sinusoidal patterns in both ACF and PACF plots

indicates that simple AR or MA processes are not appropriate for this data. Instead, the significant spike at lag 12 in both functions provides strong evidence of annual seasonality in Canadian oil production.

This correlation at lag 12 confirms our earlier observation from the decomposition analysis, showing that production follows a consistent yearly cycle. The presence of this seasonal component suggests we should incorporate a seasonal term in our model specification, likely pointing toward a SARIMA (Seasonal ARIMA) model with seasonal period  $s=12$ . The seasonal component (P,D,Q)12 will capture the annual production patterns driven by operational schedules, weather conditions, and market dynamics that recur each year.

This revelation is particularly important for accurate forecasting, as models that fail to account for this seasonality would miss systematic variations in production levels throughout the year, leading to larger prediction errors and unreliable confidence intervals. The seasonal pattern at lag 12 provides valuable information for energy market analysts and planners who need to anticipate production fluctuations for infrastructure management and market supply projections.

#### D. Naive Methods

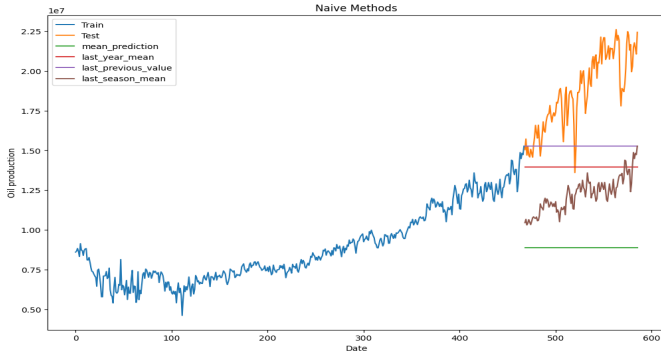


Fig. 7: Naive Methods - Mean, Last Year Mean, Last Value, Last Season

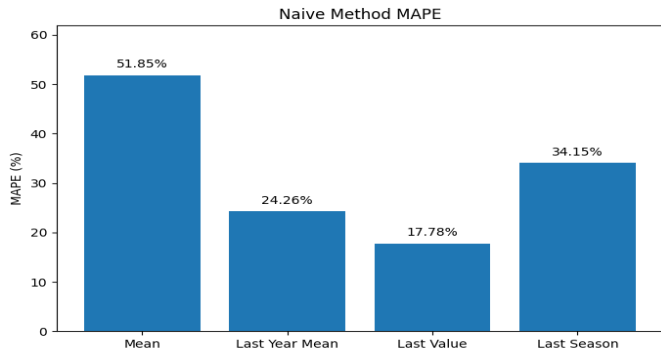


Fig. 8: Naive Methods Error - Mean, Last Year Mean, Last Value, Last Season

The bar chart compares the Mean Absolute Percentage Error (MAPE) of various naive forecasting methods. The **Last**

**Value** method yields the lowest error (17.78%), indicating the best performance among the methods. In contrast, the **Mean** method shows the highest error (51.85%), suggesting it is the least accurate. **Last Year Mean** and **Last Season** methods fall in between, showing moderate accuracy. This analysis highlights that using recent values generally improves forecasting performance.

#### E. Moving Average Model

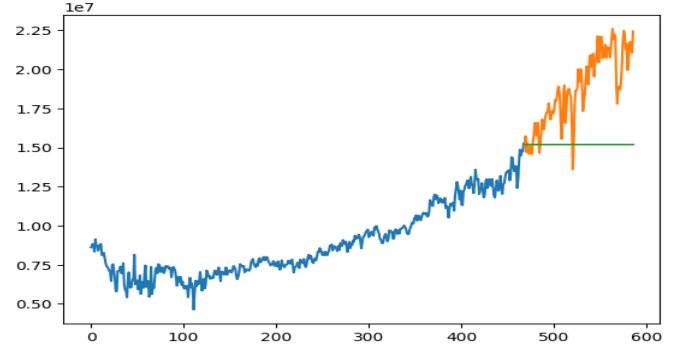


Fig. 9: Moving Average

The MA (Moving Average) model was evaluated by iterating  $q$  from 1 to 12, and the lowest test MAPE of 18.11% was achieved at  $q = 1$ . Although the error is slightly better than the AR model, the MA(1) model still shows limited predictive performance, indicating that short-term noise correction alone is not sufficient to model the data accurately.

#### F. Autoregressive Model

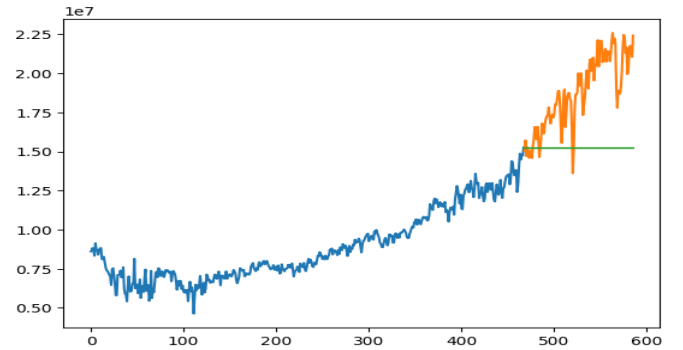


Fig. 10: Autoregressive

After iterating the AR model with orders ranging from  $p = 1$  to 12, the lowest MAPE of 18.79% was observed at  $p = 1$ . Although the prediction accuracy is limited, AR(1) was found to be the best-performing configuration among the tested models. This highlights the data's minimal autoregressive dependency.

#### G. ARIMA

The ARIMA model with order (2,1,1) was implemented to capture both autoregressive and moving average components

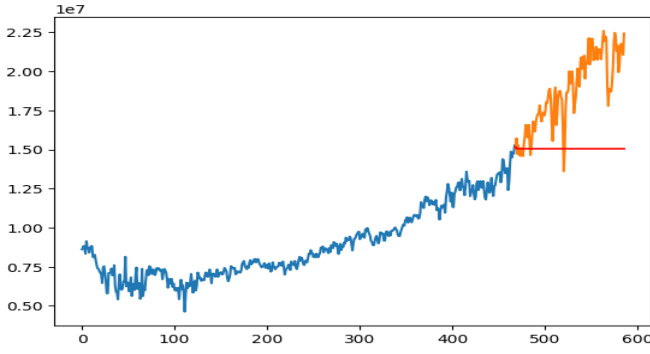


Fig. 11: ARIMA

along with differencing for stationarity. This configuration resulted in a test MAPE of 18.73% and an AIC of 13389.61, indicating moderate predictive accuracy. The inclusion of first-order differencing helped stabilize the series, while the AR and MA terms aimed to model the dependencies and noise. Despite improvements over standalone AR and MA models, the performance suggests potential for further enhancement through seasonal modeling.

#### H. SARIMA

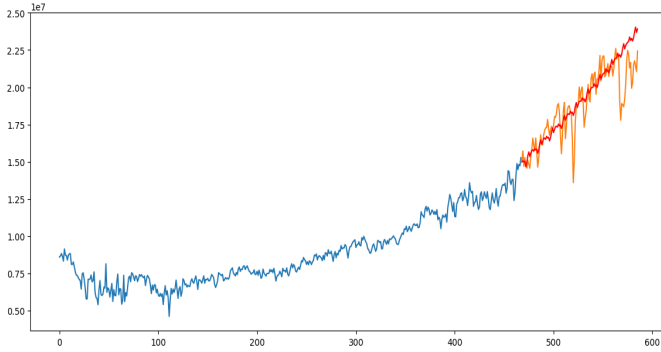


Fig. 12: SARIMA

To effectively model both non-seasonal and seasonal components in the time series data, a SARIMA model was implemented. A comprehensive grid search was conducted by varying the parameters  $p, d, q, P, D, Q$  from 1 to 3, with seasonal periods  $m = 6$  and  $m = 12$ . The model with the lowest Akaike Information Criterion (AIC) was selected as optimal, corresponding to the SARIMA order  $(1, 1, 3) \times (3, 1, 3, 6)$ . This configuration successfully captured both short-term dependencies and seasonal patterns in the data. It achieved a test Mean Absolute Percentage Error (MAPE) of **5.03%**, indicating a significant improvement over previous models. Furthermore, the optimal model yielded a minimum AIC value of **0.0028**, confirming the strong goodness-of-fit and robustness of the selected SARIMA model.

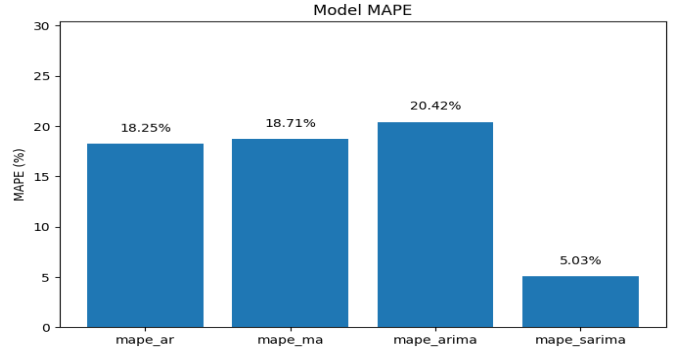


Fig. 13: MAPE comparison

#### I. Comparative Performance Analysis of Time Series Models

Figure presents a bar chart comparing the Mean Absolute Percentage Error (MAPE) of four time series forecasting models: AR, MA, ARIMA, and SARIMA. The AR, MA, and ARIMA models yielded MAPE values of 18.25%, 18.71%, and 20.42% respectively, indicating moderate prediction accuracy. However, the SARIMA model significantly outperformed the others with a much lower MAPE of only 5.03%. This highlights the effectiveness of SARIMA in capturing both short-term and seasonal patterns in the dataset, resulting in improved forecasting performance.

#### J. Gated Recurrent Unit

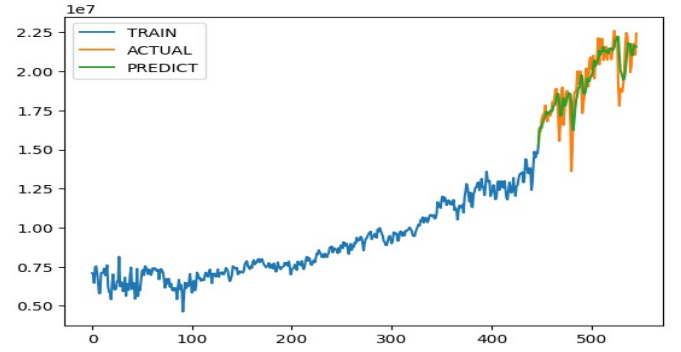


Fig. 14: GRU

To model the monthly oil production data, we employed a Gated Recurrent Unit (GRU) based deep learning architecture. The GRU model was chosen for its capability to capture temporal dependencies in sequential data while being computationally efficient. The model was trained using sequences with an input shape of  $(20, 1)$ , meaning it looks at 20 months of past data to predict the next month's production. The GRU layer was configured with 32 units and used the tanh activation function to introduce non-linearity. The Adam optimizer was utilized for faster convergence. Upon evaluation, the model achieved a Mean Absolute Percentage Error (MAPE) of 4.3%, demonstrating strong predictive performance on the given dataset.

### K. Long Short-Term Memory

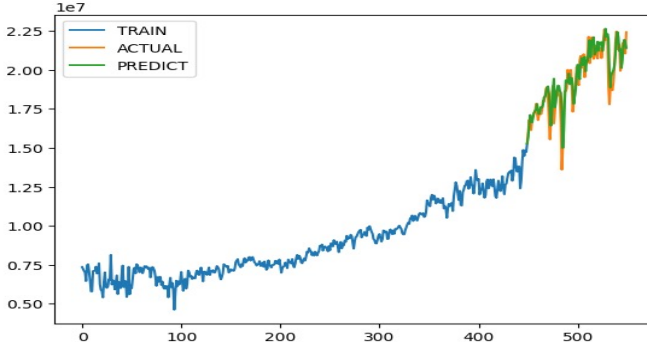


Fig. 15: LSTM

In addition to the GRU model, a Long Short-Term Memory (LSTM) neural network was also implemented to forecast monthly oil production. The LSTM architecture is well-suited for time series prediction due to its ability to learn long-term dependencies and retain relevant historical information. The model was trained using input sequences of shape (18, 1), i.e., 18 months of past data were fed into the model to predict the next month's production. The LSTM layer was configured with 32 units and employed the tanh activation function, with the Adam optimizer used for training. The model demonstrated excellent predictive accuracy, achieving a Mean Absolute Percentage Error (MAPE) of 3.57%, which indicates a high level of precision in forecasting oil production values.

### L. Recurrent Neural Network

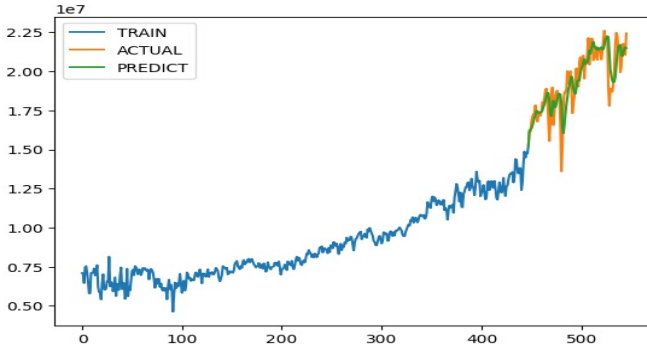


Fig. 16: RNN

A standard Recurrent Neural Network (RNN) was also utilized to forecast monthly oil production, serving as a baseline deep learning model for comparison with more advanced architectures. The RNN model was trained on sequences with an input shape of (20, 1), indicating that it considers the previous 20 months of production data for forecasting the next month. The architecture was configured with 96 units and utilized the ReLU activation function to introduce non-linearity. The Adam optimizer was selected to enhance the

model's convergence efficiency. The performance of the RNN model was evaluated using Mean Absolute Percentage Error (MAPE), where it achieved a value of approximately 4.4%, indicating a reasonably good forecasting capability despite being a simpler recurrent model.

### M. Comparative Performance Analysis of Time Series Models

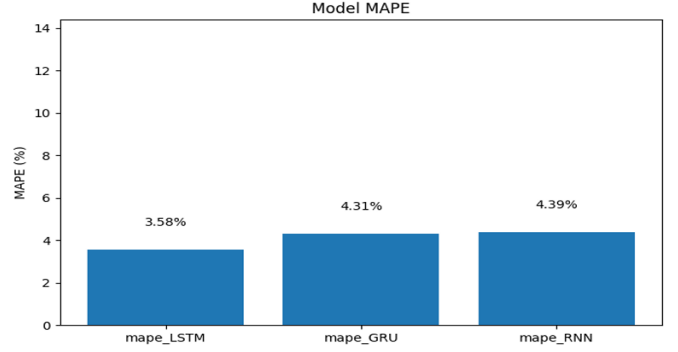


Fig. 17: MAPE Comparison

The bar chart above presents a comparative analysis of the Mean Absolute Percentage Error (MAPE) for the three deep learning models applied to monthly oil production forecasting—LSTM, GRU, and RNN. Among the three, the LSTM model demonstrated the lowest MAPE of 3.58%, indicating the highest prediction accuracy. The GRU model followed closely with a MAPE of 4.31%, while the RNN model exhibited a slightly higher MAPE of 4.39%. This visualization highlights the superior performance of the LSTM architecture in capturing temporal dependencies and producing more accurate forecasts compared to the GRU and vanilla RNN models.

### V. CONCLUSION

We focused on achieving a lower AIC for time series models and a lower MAPE for deep learning models. For time series models, we iteratively searched for the best values of  $p$ ,  $q$ ,  $P$ , and  $Q$  to obtain the lowest possible AIC. For deep learning models, we performed hyperparameter tuning to achieve the best model performance. We performed a log transformation on the time series data to reduce variance and improve model performance. After obtaining the desired output on the log-transformed series, we converted it back to the original scale and plotted the test and predicted values.